Longitudinal emittance monitoring in the Fermilab Main Injector using Intensity and RMS width sampled bunch data

Olufunmilola Ogunmefun

Supervisors
Chandra M. Bhat
Brian Hendricks

Main Injector Department, Beams Division

*Fermi National Accelerator Laboratory**

Abstract

For Run II, 36 by 36 proton and antiproton bunches will be collided in the Tevatron during accelerator operations. The probability of successful collisions is dependent on the luminosity levels achieved during the acceleration cycles. Longitudinal emittance, a measure of the phase-space area occupied by the particles in an rf bucket, directly affects luminosity. As a result, diagnosing and eliminating the emittance growth problems experienced in the Main Injector is of a high priority. The PA1896 was devised to monitor longitudinal emittance evolution in the MI for proton and antiproton acceleration cycles; The PA1925 is the updated version designed to expand data acquisition, processing, and storing procedures.

*Operated by the Universities Research Association, under contract with the U.S. Department of Energy

I. INTRODUCTION

A.Overview

The Main Injector (MI) at Fermilab is a proton/antiproton synchroton used to accelerate and inject proton and anti proton bunches into the superconducting Tevatron. It can be ramped to various energy levels depending on the operation at hand. For example, during antiproton production, the energy levels are raised from an injection point of 8GeV to 120GeV at which point, the protons are extracted and catapulted into a copper fixed target in order to produce antiproton particles; these are then stored in the accumulator ring. For proton/antiproton collision operations, the MI is ramped to 150GeV for transfer to the Tevatron. For Run II, 36 proton bunches will be collided with 36 antiproton bunches in the Tevatron with a target longitudinal emittance value of approximately 2 eV-sec at the point of collision.

Longitudinal emittance, ε_l, which refers to total phase-space occupied by the beam, directly affects luminosity and length of the luminous region in the colliding-beam systems. A higher luminosity value means that there will be more effective collisions in the Tevatron for data acquisition and analysis at the particle detector locations, CDF and Dzero. Due to this relationship between ε_l and luminosity, it is essential to monitor emittance evolution in the accelerator chain. Various studies during the course of Run II have shown a longitudinal emittance growth in the Main Injector, which is perhaps the most important accelerator in the chain as it is the site of injection into the Tevatron. Therefore, maintaining desirable ε_l levels in the MI has become a matter of importance.

Using ESME (a micro particle simulation code) simulations as well as other monitoring applications, several sources and solutions for the ε_l growth problems have been proposed. In order to test these proposals, a monitoring system, namely the console application PA1896, was devised to collect data and broadcast emittance values on the beam being ramped in the Main Injector.

The methodology of the console program is to read data from various MI ACNET SBD parameters and then, using relativisitically correct formulas, calculate longitudinal emittance. The SBD provides bunch-by-bunch data on the beam throughout the entirety of the acceleration process in the Main Injector.

The PA1896 console application gathered data from three locations along the acceleration ramp in the Main Injector for 2A, an antiproton acceleration cycle and 2B, a proton cycle at a 4 Gs/s sample rate. While this schematic provided useful values, the data acquisition was not extensive enough. As a result, the PA1925 was devised with the primary goal of gathering information for more locations in the MI and to perform emittance calculations for more peak bunches in each group. Secondary goals included investigating and fixing database storage and plotting routine problems, making provisions for a 8GS/s sample rate, as well as implementing a more coherent user interface.

B. The Proton/Antiproton Accelerator Chain

Until the decisive deviation at the Main Injector, the production process of protons and antiproton are virtually identical. The first step is the Cockcroft-Walton, a cascade accelerator which produces H^- ions by adding electron to hydrogen atoms obtained from an extensive store of hydrogen gas. Using this accelerator scheme, the ions are accelerated to approximately 750 KeV and then sent to the Linac. In this linear accelerator, the ions travel along a virtually linear path and are accelerated in a radio frequency electric field, which is synchronous with their passage through the gaps of a coaxial system of cylindrical electrodes called drift tubes. There is no field inside the drift tubes themselves so the ions are only accelerated between the gaps. The synchronous condition is created and satisfied by the fact the that the length of the drift tubes increase proportionally to the velocity of the particle. However, as the particle approaches the speed of light, relativistic modifications result in the length of the drift tubes becoming constant.

During the course of this entire process in the Linac, the H^- ions are stripped of their electrons and the protons created by this action are injected into the Booster at an energy of 400 MeV. There, they are accelerated to 8GeV and then transferred to the Main Injector. The proton bunches are extracted from the Booster in 84 buckets with 18.89 nanosecond intervals; they are then accelerated to 150GeV, which is the point of injection into the Tevatron. For antiproton production, the 120 GeV proton bunches are sent to the target every 1.5 seconds for storage of antiprotons in the Accumulator Ring. For collider operations, the stored antiprotons are delivered to the Main Injector to be ramped and then extracted to the Tevatron.

C. Transverse and Longitudinal Focusing

Transverse and phase focusing guide the beam in the Main Injector. Transverse focusing is comprised of high-order magnets such as quadrupoles that focus and defocus the beam in alternating planes as it passed through the MI tubes. Figure 1 shows the effect of these actions.

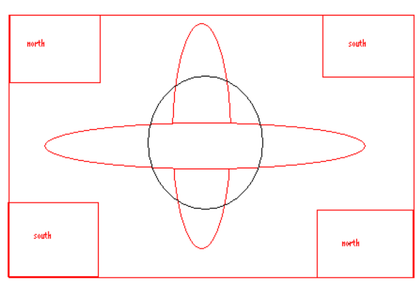

Fig. 1

A quadrupole magnet focuses and defocuses (red ellipses) the original beam (black circle).

The beam must then be refocused, or reshaped into a configuration as close to circular as possible; this reshaping is done with higher-level magnets such as sextopoles and octopoles.

The longitudinal focusing of particles is accomplished in reach radio frequency resonant cavities in the MI. These systems resonate at 588 harmonic of revolution frequency of particles in the MI. The angular frequency of the radio frequency cavity, ω_{rf} , is given by:

$$\omega_{rf} = h\omega_s = \frac{h\beta_s c}{R}$$

(eq. 1)

where β_s is the ratio of light's velocity to the that of the synchronous particle, h is the harmonic number, c is the speed of light, ω_s is the angular velocity of the particle and R is the average radius of the circular machine. The synchronous particle gains an energy dE when it reaches the rf cavity gap where:

$$dE = eV_{rf} \sin\phi$$

(eq. 2)

V represents the maximum voltage.

The particles that don't arrive at the exact location of the RF curve are called non-synchronous particles and the offset of their properties from that of the reference particle are as follows:

$$r = r_s + \Delta r, \qquad \phi = \phi_s + \Delta\phi, \qquad \theta = \theta_s + \Delta\theta$$

$$P = P_s + \Delta P, \qquad E = E_s + \Delta E$$

(eq. 3)

Therefore, the non-synchronous particles have different positions, energies, and momentum from the reference particle, thereby creating a momentum spread. So, the faster moving particles will receive a lower energy kick, which results in them receiving less acceleration than the slower moving particles that arrive at a higher level of the RF wave. In this manner, the particles become grouped together in what it is referred to as a bunch; the behavior of the particles in the bunch is called synchrotron oscillation because the non-synchronous particles are oscillating about the reference particle due to their space and momentum fluctuation. For small $\Delta\phi$ and ΔE, the oscillation frequency is [2] :

$$f_{syn} = \left(- \frac{eh\eta_0 V_{rf}\cos\phi_s}{2\pi\beta_s^2 E_s} \right)^{1/2} \frac{\omega_s}{2\pi},$$

(eq. 4)

This oscillation forms a Hamiltonian contour around a stable $\Delta x - \Delta p$ area called a bucket. The number of buckets is equal to the harmonic number.

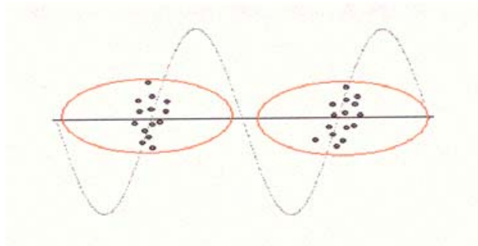

Fig. 2

The particles, shown in black, form a bunch inside an rf bucket (red ellipse).

The Main Injector uses three RF systems: 2.5 MHz with harmonic number 28, 5 MHz with harmonic number 56, 53 MHz alternating voltage for which the corresponding harmonic number is 588 and the bucket length is 18.87nsec. For Run II, the antiproton beam arrives in four groups, also referred to as a shot. The total length of an antiproton shot is 84 buckets. The proton beam arrives in one group which makes up the proton shot.

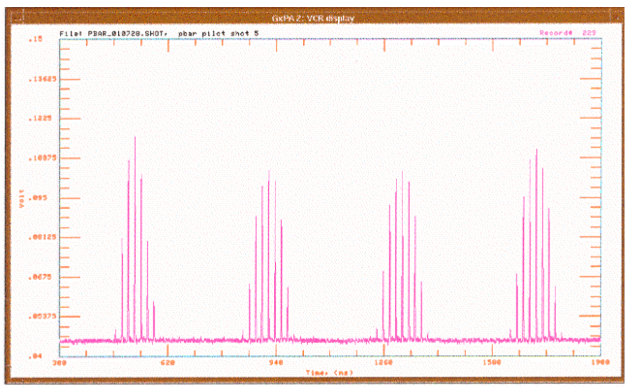

Fig. 3

An antiproton shot comprised of 4 groups, each with 7 to 9 bunches.

II. LONGITUDINAL EMMITANCE GROWTH IN THE MI

Longitudinal emittance is the total phase-space area occupied by the particles in a bucket. It can be expressed in terms of bunch length, RF voltage, and synchrotron energy. The ε_l formula used by the console application is:

$$h := 588 \qquad \gamma t := 21.836 \qquad Es := KE + mp \qquad \gamma := \frac{Es}{mp} \qquad \eta := \frac{1}{\gamma t^2} - \frac{1}{\gamma^2}$$

$$\varepsilon l := \sqrt{32} \cdot \sqrt{\frac{Vrf \cdot R^2\, Es \cdot 10^9 \cdot 10^6}{2 \cdot \pi \cdot h^3 \cdot c^2 \cdot |\eta|}} \cdot \int_0^Q \sqrt{\cos(x) - \cos(Q)}\, dx$$

(eq. 5)

Where V_{rf} is the rf voltage, R is the radius of the accelerator, h is the harmonic number, C is the velocity of light, γt is the relativistic gamma at transition, η is the momentum compaction factor and Q is half the bunch length expressed in radians. The following are the major causes of emittance growth in the Main Injector.

A. Injection Oscillation/Phase Mismatch

When transferring the beam of particles from one accelerator to the next, the goal is to inject the particles at the proper position to situate the beam in the central orbit so that there is no impact on the particle distribution. In order to achieve this, both the position and the angle of injection must be in perfect accordance with that of the central orbit. The problem of injection oscillation arises when these conditions are not met. If the angle is off by any number of degrees, a phase mismatch develops whereby the non-synchronous particles will arrive at the wrong section of the rf wave and will not be captured properly to maintain the right oscillation around the synchronous particle. As a result, the radius of their oscillation period increases causing the bunch to occupy more bucket area; eventually, the injection oscillation disappears but only at the price of emittance dilution.

B. Bunch Coalescing

Bunch coalescing in the Main Injector is a process whereby several 53MHz bunches are merged into a single 53 MHz bunch. This is accomplished by capturing a group of 53 MHz bunches into one 2.5 MHz rf bucket; the bunches are then allowed to complete a quarter synchrotron oscillation, ¼ t_s, which results in an approximately linear organization. At this point, the bunches are then recaptured in a 53 Mhz bucket. The following is an illustration [1] of the coalescing process.

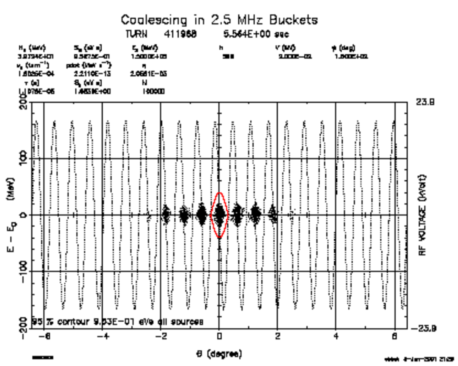

Fig. 4.1

7 bunches are stored in 53MHz buckets at the beginning of the coalescing process

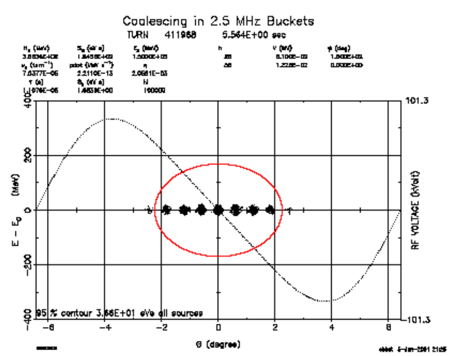

Fig. 4.2

The 53MHz rf is replaced by a 2.5 MHz rf wave.

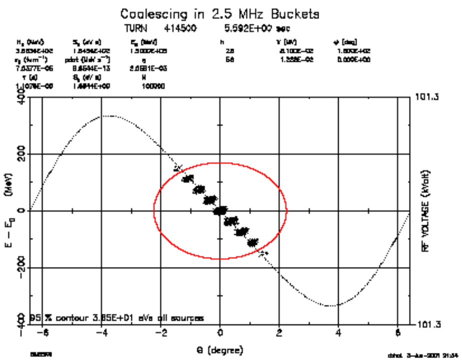

Fig. 4.3
Bunch rotation commences; one-eight synchrotron oscillation (1/8 t_s)

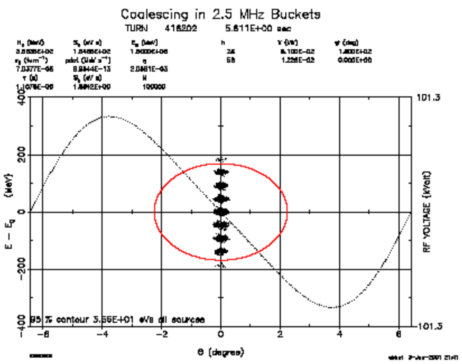

Fig. 4.4
One-quarter synchrotron oscillation, 1/4 t_s

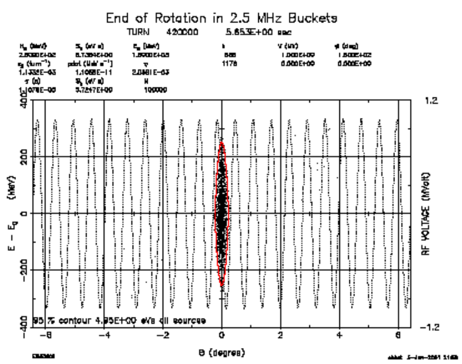

Fig 4.5
At ¼ ts, the 53 MHz rf voltage wave is reapplied; now all the seven bunches are captured in one bucket

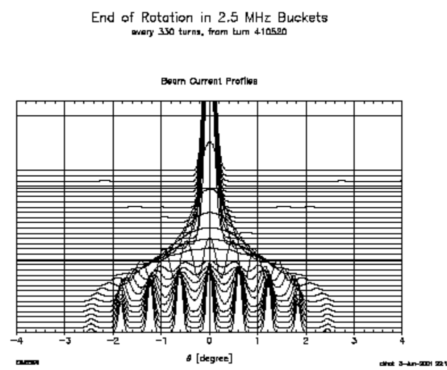

Fig 4.6
A pictorial representation of bunch coalescing in the MI.

Emittance growth problems during coalescing arise primarily from the bunch rotation portion of the overall process. If the momentum spread of the particles within the bunches are not properly accounted for, some of these particles will lag behind during rotation because their synchrotron oscillation period is longer. This behavior results in a distortion of the coalesced bunch into an 'S' configuration which engenders beam loss in the MI.

C. Transition Crossing

During acceleration in a synchrotron such as the Main Injector, when $\gamma t = \gamma s = \alpha_0^{-1/2}$ the phase-slip factor, η_0 changes sign. γ_s is the ratio of the energy of the synchronous particle E_s to E_o, its rest energy. α_0 is the momentum compaction factor, a lattice parameter which measures the fractional charge in orbit length $\Delta C / C_s$ for each unit fractional deviation in particle momentum δ. This acceleration instant is referred to as transition crossing and $\gamma_t E_0$ is the transition energy.

During acceleration before transition, the non-synchronous particles experience the same unit acceleration as the synchronous particle due to the synchrotron oscillation; additionally, this oscillation of the particles within the bucket exists only in adiabatic time.
Bucket height has the property,

$$(\Delta E)_{\text{bucket}} \propto \left(\frac{E_s}{|\eta_0|} \right)^{1/2}$$

(eq. 6)

where η_0^{-1} changes rapidly around transition. Assuming that the rate of change of γ_s is constant near transition,

$$\frac{\Delta C}{C_s} = \alpha_0 \delta.$$

(eq. 7)

gives

$$\eta_0 = \frac{2\dot{\gamma}_s t}{\gamma_s^3}.$$

(eq. 8)

Time t is measured starting from the instant when the synchronous particle crosses transition. As particles approach transition, the synchrotron frequency gets reduced to zero while bucket height approaches infinity according to eqs. 4 and 6. The period where the synchrotron oscillations are virtually frozen is called non-adiabatic time. As a result of this phenomenon, there will be an interval when phase focusing is zero. For the MI, non-adiabatic time lasts for 2.1 msec. During the period of non-adiabatic time, momentum spread increases rapidly, and could exceed the momentum aperture of the accelerator; this leads to significant beam loss.

Another characteristic of transition crossing is that different beam particles in a bunch cross transition at varying times. Therefore, depending on the momentum spread, a particle with peak momentum δ (where δ is equal to $\Delta p/p$) crosses transition earlier than the synchronous particle by a time period called non-linear time.

During this time some particles are above transition while others are below. If the rf transition phase jump is set at the time where the synchronous particle is engaged in transition crossing, those higher momentum particles that have already crossed transition will spend a significant period of time above transition before the rf phase jump. As a result, these particles will be subjected to a non-linear force that moves them along hyperbolic divergent paths. The particles with a lower momentum than the synchronous particles experience a non-linear force once the rf phase jump is initiated and they will also move along divergent paths. This dual action produces two tails in the phase-space distribution within the bucket. This in turn results in emittance growth.

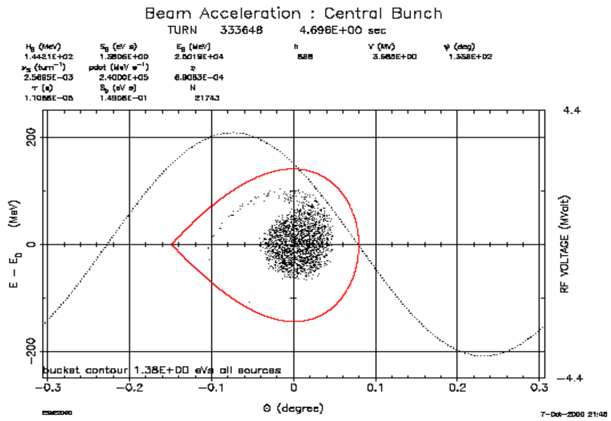

Fig. 6

Results of non-linear force on off-synchronous momentum particles

Most of the longitudinal emittance dilution in the Main Injector for very intense bunches with bunch intensity greater than 10^{11} particles are a result of transition crossing. Typically, the MI accelerates $6x10^{10}$ particles per bunch; therefore, transition crossing problems can be mostly avoided.

In order to develop viable means of reducing beam loss in the MI from RF voltage mismatch and bunch coalescing, a mechanism by which ε_l can be measured and analyzed becomes extremely important. This is where the PA1925 comes in. By taking more longitudinal emittance data, the Main Injector group aims to effectively analyze the evolution of this essential beam property during transition in particular, and the entire acceleration process in general.

III. THE PA1925 CONSOLE APPLICATION

A. Accelerator Controls System, ACNET

PA1925, like all other console applications operating at Fermilab, is dependent on ACNET, the acronym for the Accelerator Control NETwork. ACNET can be thought of in two different ways: 1. As the entire system of computers, links, and software required for the monitoring and control of all the accelerators [3] and (2) as a software communications package by which the central computers, front ends, consoles and other subsystems communicate. Front ends are computers that directly interface with the various accelerator hardware; it is at this junction that data acquisition and hardware control occur. Console applications are the human interface to accelerator control. They are used by the operators in the MCR to run the accelerator chain here at Fermilab after they have been developed and tested by programmers by way of an in-house testing environment. All source code information is evaluated and stored by MECCA (Management Environment for Controls Console Application) as a means of preserving all operations-critical material for future reference.

B. Sampled Bunch Display, SBD

The Main Injector Sampled bunch display, MI SBD, displays sampled data regarding each bunch in the MI. This data includes intensity, longitudinal bunch width, and RMS sigma. All of these are bunch properties integral to the calculation and data analysis process of the console application. The MI SBD consists of a Lecroy 2.8 GHz oscilloscope (it is a resistive wall beam signal pick up monitor) and the data handling system called Labview. The Lecroy device takes raw data from 25 beam detectors in the accelerator process specified by the user and then Labview uses this information to calculate and broadcast scaled intensity, longitudinal bunch width, and sigma values for each bunch. For the PA1925, data will be obtained from 7 different time points on the beam that is currently being accelerated.

C. Data Acquisition parameters and modes

For any data acquisition in ACNET, a programmer must specify data parameters, which represent the name of a particular device. The primary parameters used for the PA1925 are listed and described in the following table.

DEVICE NAMES	STRUCTURE	PURPOSE
I:SBD01-07**I**	Each devices provides an array of 676 elements, each corresponding to an rf bucket. Usually, the necessary data is stored in the first 84 elements of the array.	These devices contain bunch intensity readings for the program's 7 beam monitoring locations: MI Injection, Flattop, Pre-Acceleration, Pre-Transition, Post-Transition,Flattop, End-of-coalescing, and Extraction.
I:SBD01-07**W**	Each devices provides an array of 676 elements, each corresponding to an rf bucket. Usually, the necessary data is stored in the first 84 elements of the array.	These devices contain RMS bunch length (95% width) readings for MI Injection, Flattop, Pre-Acceleration, Pre-Transition, Post-Transition,Flattop, End-of-coalescing, and Extraction.
I:SBD01-07**W**	Each devices provides an array of 13200 elements; the number of elements that are available at any given time varies with the sample rate being used by the front end devices. For the most part, a 4GS/s sample rate will be used; this rate corresponds to approximately 3600 array elements.	These devices contain raw data readings for MI Injection, Flattop, Pre-Acceleration, Pre-Transition, Post-Transition,Flattop, End-of-coalescing, and Extraction. These values can either be negative or positive depending upon the device location with respect to transition; they are a mesaure of the amplitude of the beam in the various rf buckets.
I:SBDMOM	This device gives an array of 25 elements. For this program only the first seven elements will be used for emmitance calculations.	Provides a one-shot momentum reading for the current ramping scheme.
T:STORE	Single-reading devce	Provides and identificaiton number for the data acquired from a specific acclerator run store

Table 1

There are various MI modes available for data collection; for the purposes of this program, two modes, namely 8 and 9 have been created for emittance monitoring. Mode 8 is set to 2B, a proton acceleration cycle, in combination with trigger event 15, an MI reset event. Mode 9 is set to 2A, an antiproton acceleration cycle, in combination with trigger event 9A, another MI reset event. For simple testing, once can also use a mode 10, which represents a stacking cycle (antiproton production) and is a combination of 29 and 1F.

D. Program Modules

The console application is comprised of three main modules, Live Capture, Graphing, and Data Retrieval.

1. Live Capture

This module uses an event callback sequence to monitor the beams in the Main Injector; once the user starts it, the module will repeatedly procure data at the seven locations on the beam. Each shot's five central bunches are located; subsequently, emittance and intensity data are read, processed, and then displayed on the console screen. This process is repeated for 9 shots after which the user can save the data for future reference or email the corresponding raw data values to his or herself (one can also stop the data collection at any point and then store the data at anytime).

2. Graphing

Each time a shot is being processed by the Live Capture routine, there is a simultaneous acquisition of raw data values for that particular shot. After the intensity and emittance values have been displayed on the screen, the graphing module plots out two screens of seven graphs, each depicting amplitude vs. time. Under the replot option on the main menu bar, one can also shift the plot horizontally as well as enlarging or shrinking the size of the plot.

3. Data Retrieval

This module displays the emittance data stored by a previous Live Capture execution. Like the Live Capture display schematic, this module allows the user to alternate between the 7 different data display screens, each representing a particular beam monitoring location.

The other routines in the program serve to provide important MI beam cycle information to the user. For example the Mode Settings window, which is first to be displayed by the program, provides information on the cycle to be monitored. The following figures are screen shots of the various windows available to the user.

E. Data Samples

The following program samples were taken from a 2B accelerator cycle.

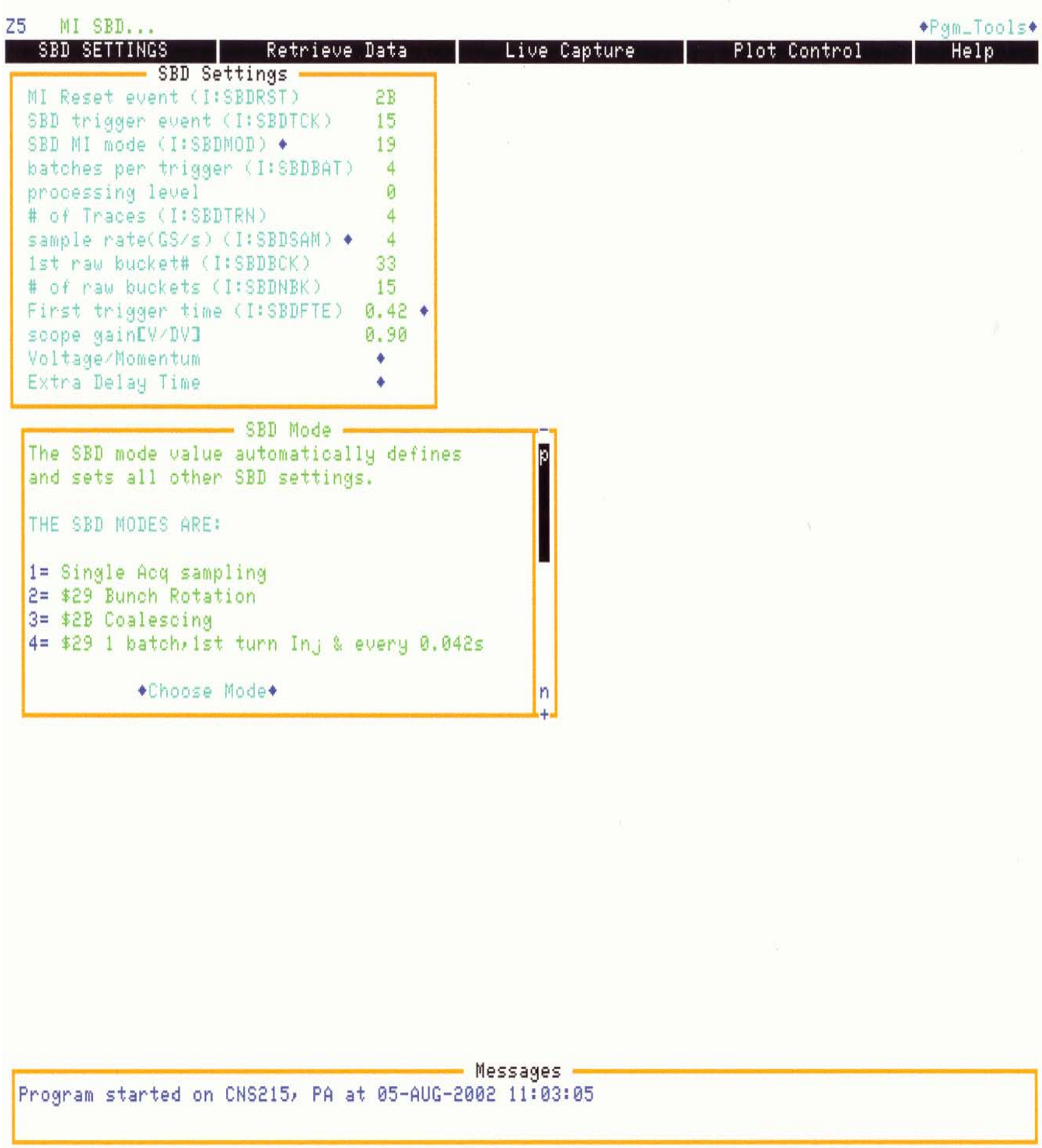

Fig. 7

The SBD settings window is displayed upon initialization of the program. It displays all the vital information about the set accelerator mode for the Main Injector and allows the user to change the oscilloscope sample rate, view the voltage, momentum, and acquisition time values. The SBD mode window allows the user to change the MI mode. The message window displays important program information to the user.

Fig. 8

This is a screen image of the Live Capture window after the end of a 2B data acquisition sequence; the user is given the option of storing data and/or emailing the raw data values to his/her email account. For a 2B cycle such as this, all the information comes in the first group. The top row displays longitudinal emittance values; the bottom row displays bunch intensity values. The bunch width display table shows the bunch width values for the central peak bunches.

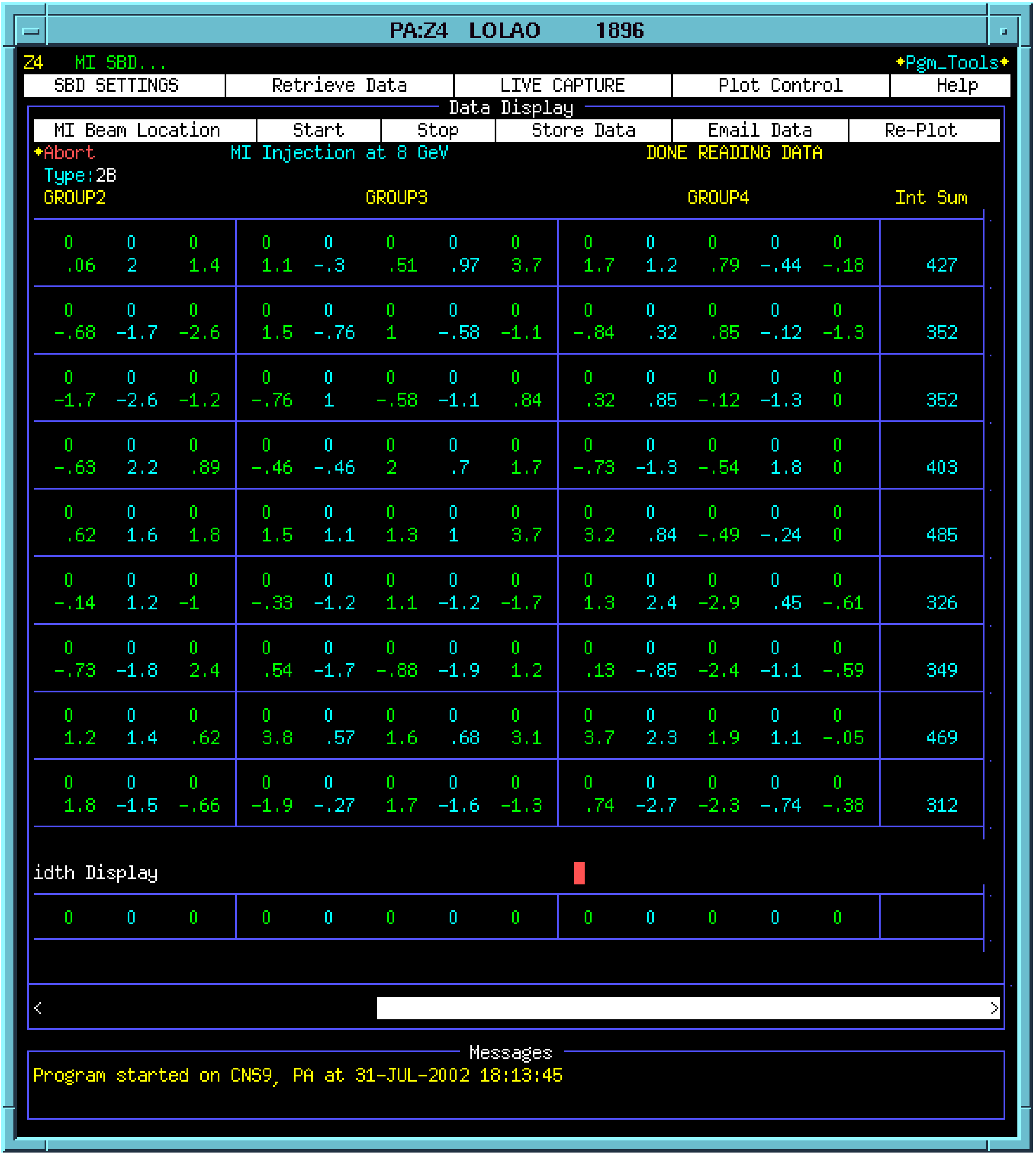

Fig. 9

Main Control Room screen shot of a 2B cycle. The window has been scrolled to the end of the screen. The last column displays the intensity sum for the entire shot.

IV. RESULTS/CONCLUSION

During the first trial runs of the PA1925, a few problems arose with the raw data values from the 4 devices that were storing data above transition energy. In order to correct these problems, a data-scaling scheme was devised to appropriately adjust the values to match those from the devices positioned below transition. There were also concerns over background "ghost" data in the raw data buffers; however, the problem can only be fixed by some form of an SBD front-end checkup. The database reading/writing routines were adjusted to accommodate the increase in data acquisition; the help and mode information windows were expanded to provide more information for the user.

At the beginning of this program update, one of the main problems was that the program appeared to be reading old data from the device buffers. This problem was addressed by reading the end-of-beam times from the Abort Clean-Up devices for the Main Injector and allowing the user to add a finite amount of delay time (default is 3 seconds) to those values. This delay sequence allows Labview enough time to process the new data; therefore, the data acquired by the program will be that corresponding to the current beam.

The console application has since been moved to the W (working) console page to be tested for controls operator usage. It is entry W41 under the title "MI SBD Emmitance2".

Subsequent testing of the updated PA1925 has shown it to be an important diagnostic tool for monitoring longitudinal emittance in the Main Injector. The next step in the evolution of this console application would be to further expand the beam monitoring locations along the ramped beam and to evaluate the program's execution during an 8 Gs/s sample rate run. Overall, the console application is expected to become integral to accelerator operations for the Main Injector group during the remainder of Runs II and IIb.

ACKNOWLEDGEMENTS

Thanks to my supervisors, Chandra Bhat and Brian Hendricks of the Beams Division for their continued assistance during this process. Additional thanks are due to Robert Flora of the Instrumentation department as well as Elliott McCrory and Jay Dittman of the SIST program. I would also like to express my sincere gratitude to Dianne Engram and Dr. James Davenport for all their support and understanding.

REFERENCES

[1] C.M. Bhat. Antiproton coalescing at 150 GeV ESME simulation. Febuary 8, 2000.

[2] C.M. Bhat et. al., "Transition crossing in proton synchrotrons using a flattened rf wave." Phys. Rev. E 55, 1 (1997), pp 1028-1034.

[3] "Controls Rookie Book", 3rd Ed. Printed July 16, 2002.

[4] C.A. Rodriguez and C.M. Bhat, "Pbar Acceleration in the Main Injector for Run II: ESME Simulations." August 2000.

[5] K. Danquah, "Online longitudinal emittance monitoring in the Main Injector for Collider operations." August 2001.